Materials Chemistry and Physics 301 (2023) 127636

Contents lists available at ScienceDirect

Materials Chemistry and Physics

journal homepage: www.elsevier.com/locate/matchemphys

Physical, chemical, and biological characterization of biodegradable chitosan dressing for biomedical applications: Could sodium bicarbonate act as a crosslinking agent?

Julia Vaz Ernesto [a], Ísis de Macedo Gasparini [a], Fúlvio Gabriel Corazza [a], Mônica Beatriz Mathor [c], Classius Ferreira da Silva [b], Vania Rodrigues Leite-Silva [a], Newton Andréo-Filho [a,*], Patricia Santos Lopes [a]

[a] Universidade Federal de São Paulo, Instituto de Ciências Ambientais, Químicas e Farmacêuticas, Departamento de Ciências Farmacêuticas, Diadema, SP, Brazil
[b] Universidade Federal de São Paulo, Instituto de Ciências Ambientais, Químicas e Farmacêuticas, Departamento de Engenharia Química, Diadema, SP, Brazil
[c] Energy and Nuclear Research Institute, IPEN/CNEN-SP, Brazil

HIGHLIGHTS

- Chemical cross-linking of chitosan scaffolding may be dispensable.
- Chemically non-cross-linked scaffolding provides greater risk-benefit advantage.
- Easy-to-handle reagents to create a green biodressing.
- Safe biodressing with low cost.
- Cell adhesion and degradable biodressing.

GRAPHICAL ABSTRACT

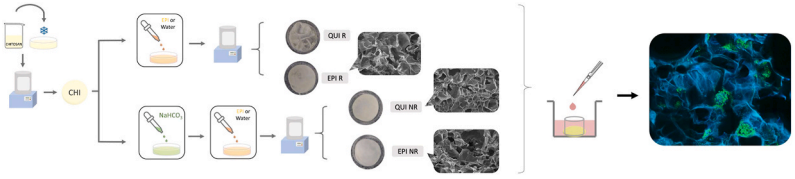

ARTICLE INFO

Keywords:
Sodium bicarbonate
Physicochemical characterization
HaCat
L929
Wound healing

ABSTRACT

Chitosan, a biomaterial with properties that allows the elaboration of biocompatible and biodegradable systems, was employed to prepare dressings - 2% (w/v) in acetic acid - followed by freezing and lyophilization. Some samples were kept chemically unchanged and used as control, while others were cross-linked with Epichlorohydrin 0.01 mol L^{-1} for 24 h being washed, frozen and lyophilized. The neutralization procedure was performed with sodium bicarbonate, which ended up leading to a crosslinking by ionic interactions in the polymer network, and characteristics as promising as those of the chemically cross-linked with Epichlorohydrin. SEM showed that the crosslinking leads to a controlled formation of the polymeric network, conferring suitable steam permeation capacity 107 g $mm.day^{-1}.m^{-2}.kPa^{-1}$, simulated fluid permeation between 2000 and 2500 g m^{-2}.day-1 and porosity with interconnection which allows fluid absorption capacity above 900%. The crosslinking processes favored a better handling mechanical resistance confirmed by biodegradation assays. The dressing blocked micro-organisms permeation, forming an efficient barrier against contamination, is safe and biocompatible, allowing satisfactory cell adhesion and proliferation. These results showed that both dressings present statistically and satisfactory equivalent characteristics to be used as a functional bio dressing suitable for the treatment of different pathologies.

* Corresponding author. Rua São Nicolau, 210 - Centro, Diadema, São Paulo, SP - CEP: 09913-030, Brazil.
E-mail addresses: juliavaz_e@hotmail.com (J.V. Ernesto), gasparini.isis@gmail.com (Í.M. Gasparini), fcfulviocorazza@gmail.com (F.G. Corazza), mathor@ipen.br (M.B. Mathor), cfsilva@unifesp.br (C.F. Silva), vania.leite@unifesp.br (V.R. Leite-Silva), newton.andreo@unifesp.br, andreonf@hotmail.com (N. Andréo-Filho), patricia.lopes@unifesp.br (P.S. Lopes).

https://doi.org/10.1016/j.matchemphys.2023.127636
Received 14 November 2022; Received in revised form 12 March 2023; Accepted 13 March 2023
Available online 22 March 2023

1. Introduction

Obtaining materials made with renewable and bioabsorbable components, such as natural polymers, which have properties equivalent to that of synthetic products [1], has attracted interest in the regenerative medicine due to the flexibility of chemical manipulation and decomposition capacity in low molecular weight fragments that can be eliminated by the human organism [2].

Chitosan and its complexes have been studied for several biomedical applications a restorative and healing agent, due to chitosan property of increasing the functions of inflammatory cells, promoting cell organization, and acting in the repair of large wounds [3].

However, for the application of chitosan in the production of biomaterials, it is necessary to modify it in order to improve mechanical properties [2,4]. Chemical crosslinking is a direct method to produce permanent networks between polymer chains, with groups -NH_2 and –OH of chitosan, active sites capable of forming these bonds [4]. However, the choice of crosslinking agents should be careful, since many are associated with cytotoxicity [1,5–7].

Epichlorohydrin (C_3H_5ClO) was chosen as a crosslinking agent since it does not eliminate the cationic amine groups of chitosan, and such groups may represent potential points of interaction with the cells that are intended to be incorporated into the dressing systems. In the reaction of crosslinking with Epichlorohydrin, the rupture of the epoxy ring and removal of chlorine from Epichlorohydrin results in carbon atoms that bind to the chitosan hydroxyl groups of carbon 6 [8].

Aqueous dispersions obtained by mixtures of chitosan particles freeze-drying has been widely explored due to the relationship of the technique with the achievement of materials with high porosity and interconnectivity of desirable pores [9]. It is known that chitosan is insoluble in neutral and basic aqueous solutions, and soluble in acidic aqueous solutions (pH less than 6.2), due to the fact that solubilization is promoted by protonation of the free amine groups of the polymer chain [1,6]. Consequently, dressings made with this polymer often require final sample pH neutralization to ensure cytocompatibility. Although it is a necessary step before the rehydration of polymeric matrices, there is still little information regarding the effects of neutralization by different methods on the physicochemical properties and cytocompatibility of chitosan [10].

Although NaOH is the most widely used neutralizing agent, there are reports in the literature showing that its use compromises the structural integrity of the material leading to the formation of residual particles [9,11]. This fact encourages the search for another reagent such as Sodium bicarbonate ($NaHCO_3$) that is a weak base, which can be used to neutralize the acidic chitosan solution. The reaction between HCO3- and H +, will produce carbon dioxide (CO_2) and water (H_2O), resulting in an increase in pH, generating the balance via carbonic acid, as well as between the protonated amino saccharides units of chitosan, and the deprotonated ones [11].

Ionic interactions occur between the protonated chitosan amine groups (positively charged), and negatively charged molecules [6,11]. Secondary interactions, such as hydrophobic interactions and hydrogen bridges between the hydroxyl groups of chitosan and ionic molecules, or interactions between deacetylated units of chitosan chains after neutralization of the amine groups improve the mechanical properties of the material [4,6].

Although the use of $NaHCO_3$ in hydrogel has been reported [11,12], dressings structured by sodium bicarbonate were not found in the literature due to the “crosslinking like” effect produced by physic junctions. The preparation of chitosan materials with ionic bonds avoids the use of catalyst or toxic crosslinking agent, which is an advantage for biomedical applications [5].

In this context this work explores the development of chitosan biodressings obtained by freeze-drying to obtain reticulated and porous structures. Physicochemical characterization tests were performed to investigate whether the properties of the dressing resulting from each treatment would be preserved and comparable in the final structure. In addition, biological, mechanical and water vapor and fluid transmission tests were performed to evaluate the use of these structures as a biodressing.

2. Materials and methods

2.1. Materials and casting solutions

Chitosan extracted from shrimp shell was supplied by Polymar (Ceará, Brazil). The polymer presented molar mass of 1.47×10^5 g mol^{-1}, measured using gel permeation chromatography with a refractive index detector [13], and the degree of N-acetylation was 22.30%. Chitosan was dissolved in acetic acid [1% (v/v)] to prepare a 2% (w/v) solution. The sodium hydroxide (NaOH, P.A, Dinâmica), sodium bicarbonate ($NaHCO_3$, P.A, Synth) and Epichlorohydrin (99%, Fluka Analytical) solutions were prepared using deionized water. Phosphate-buffered saline (PBS) solutions at pH 7.4. Simulated wound exudate fluid (SWEF), a sodium chloride (Synth C1060. 01AH lote:178580) and calcium chloride (P.A, Nuclear lote:15100942) solution containing 39 mmol L^{-1} of sodium ions and 3,6 mmol L^{-1} of calcium ions (adapted from Thomas [14]).

2.2. Preparation of the dressings

Chitosan solutions 2% (w/v) were agitated by 2 h and 0.35 g cm^{-2} were cast on polystyrene plates. After frozen at −20 °C by 24 h, the samples were freeze dried (Liobras Liotop L108), −60 °C and 40 mmHg by 48 h. The first cycle of freeze drying was common to all samples, identified as “CHI".

The 0.01 mol L^{-1} epichlorohydrin crosslinking solution solubilized in 0.28 g NaOH in purified water was used to prepare EPI R. The samples were immersed in the solution 0.35 mL cm^{-2} for 24 h, and then washed with deionized water for three times. Control samples identified as “QUI R″ were submitted to the whole process, however they were submerged in ultra purified water, without any alkaline epichlorohydrin solution or sodium bicarbonate solution.

A neutralization procedure was added prior to the chemical crosslinking treatment in “EPI NR” samples, exposing the samples to the 0.1 M solution of sodium bicarbonate in water for 30 min, followed by three consecutive washes with ultra-purified water, and continuing with the crosslinking as explained previously. The “QUI NR” samples were exposed to water after neutralization with $NaHCO_3$ for 24 h. All samples were freeze dried again after the treatments.

2.3. Physicochemical characterization

The FTIR spectra of the samples were recorded with an Infrared Prestige-21 spectrophotometer (Shimadzu) at wavenumbers ranging from 4000 to 400 cm^{-1} at 2 cm^{-1}. The pellets were prepared by homogenous mixtures of KBr and powder of each sample compression in flat-faced punches.

The sample morphology was observed by scanning electron microscopy (SEM) at 10 kV of voltage and 100pcA (JEOL - JSM-6610 LV). Prior to SEM analysis, the dressings were freeze-dried in liquid nitrogen and coated with gold in Sputter Coater SC 7620. The final structure of the matrix on the longitudinal surface and the cross-sectional area of rupture were analyzed.

Differential scanning calorimetry (DSC) of the samples (~2–3 mg) was performed under a nitrogen atmosphere with a DSC-60H (Shimadzu) with a flow of 100 mL min^{-1} at a heating rate of 10 °C.min^{-1} and temperature ranging from 25 to 550 °C.

The thermogravimetric analysis (TGA) of the samples (~4–6 mg) were performed at TGA-60 (Shimadzu) under a nitrogen atmosphere with a flow of 100 mL min^{-1}, a heating rate of 10 °C/min and temperature ranging from 30 to 700 °C.

2.4. Water vapor permeability

As previously described by Leceta, Guerrero, & Caba [15], water vapor permeability (WVP) of the samples was determined according to ASTM E96-00 (ASTM, 2000). The samples were cut into a circle of diameter 3 cm and placed on the top of the cylindrical cup [test area of 15.02 cm^2 (S)] containing silica gel. The system (cups with samples) was incubated in a desiccator with 75% relative humidity, containing saturated saline solution, and maintained at 37 °C for 24 h. The systems were periodically weighted within 2 h. The WVTR was calculated as the following equation.

$$WVTR = \frac{G}{t\ x\ A}$$

where G is the change in weight (g), t is the time (h), and A is the test area (m^2). WVP was calculated as:

$$WVP = \frac{WVPR\ x\ T}{\Delta P}$$

where T is the thickness of the test specimen (mm), and ΔP is the partial pressure difference of the water vapor across the dressings. WVTR and WVP of three specimens for each sample were calculated and reported.

2.5. Simulated Fluid Handling Capacity and swelling degree

Simulated fluid permeation (PFS) was determined using the standardized method of relative humidity gradient equal to 75%, adapted from Thomas [14]. Quadruplicates of each sample were cut into discs of diameter 3 cm, weighed on an analytical balance (Shimadzu model AY220), and coupled to PVC apparatus for analysis, an adaption of the "Paddington cup", containing SWEF.

The samples were positioned with the nozzles facing down, providing the interaction of the fluid with the samples. They were arranged in an airtight chamber, containing silica gel (Synth D10 10. 08AH lot:177687) and kept at 37 °C for 24 h. The mass of the sets was monitored at the beginning and end of the assay. The samples were decoupled from the systems, and the final mass of these systems was also measured. The results are obtained from the change in mass of the systems indicating the difference in fluid volume inside them after the given period, and also by the change in the mass of the samples alone.

The results of this experiment lead to the permeation rate calculus of the fluid of the samples, the fluid absorption capacity of these samples, and the fluid movement capacity in $g.day^{-1}.m^{-2}$.

The swelling degree was measure in three different solutions. Dried samples were weighted (Wd) and then incubated at 37 °C for 24 h in phosphate-buffered saline (PBS), or culture medium enriched with 10% bovine fetal serum (D10), or SWEF. Samples were removed from the solutions, and the weight recorded (Ww). Swelling degree of dressing samples was obtained from the following equation:

$$Swelling\ degree\ (\%) = (W_w - W_d) / W_d * 100$$

Triplicates of the samples were weighed on an analytical balance (Shimadzu model AY220). The equivalent of 40 times the mass of each specimen of simulated fluid (solution containing calcium chloride and sodium chloride) heated to 37 °C was added over them. The scaffolds were taken to an oven at 37 °C. To assess dehydration, their masses were measured every 10 min for a period of 210 min from the beginning of the test. A final measurement was taken after 24 h (W_f). The gel fraction (GF) calculation was performed according to Stanescu et al. [16]:

$$GF\ (\%) = \frac{W_f}{W_d} * 100\%$$

2.6. Mechanical tests

The mechanical resistance analysis was performed in a TA-CT3 50K Texturometer (Brookfield, Middleboro, MA 02346, USA) to determine the parameters of rupture force and distance or displacement of rupture, used in compression mode, with the cylindrical probe of diameter 2.0 mm TA39.

The thickness of five points of each sample was measured. The circular samples of approximately of diameter 3 cm were pre-packaged or maintained for 48 h in a desiccator containing saturated sodium chloride solution (Synth, Diadema, Brazil), which promotes 75% relative humidity.

The samples were fixed by the ends in adapted support so that a disc of diameter 2.6 cm was exposed to the test, and that the force was applied in the center of the circle and perpendicular to the dressings. The samples were submitted to perforation with the probe at a speed of 1 mm/s moving until rupture. The maximum force of the peak was recorded as a rupture force, and the distance to the equivalent peak was recorded as distance or rupture deformation.

2.7. In vitro biodegradation

The biodegradation rates of the dressings were compared, samples of 1.4 cm^2 were cut and weighed on an analytical balance. Triplicates of each sample were immersed in PBS, with physiological pH 7.4 containing human lysozyme (Sigma-Aldrich ≥100,000 U/mg) at concentration 0.1 mg/mL [17,18] on PBS without the enzyme for comparison. The tubes containing the samples were kept at a temperature of 37 °C. The time intervals chosen were 2, 5, 7, 14, 21, and 28 days. The degradation degree was expressed by the samples weight loss percentage after freeze-drying in each evaluated time, remained mass of the dressings, in relation to the initial weight (Wi) of each one. The degradation rate was calculated according to the equation:

$$Biodegradation\ rate\ (\%) = (W_i - W_r) / W_i * 100$$

2.8. Biological assays

The samples were previously decontaminated by exposure at UV radiation for 30 min each side. They were cut into a disc shape of 1 cm or 5 cm diameter using a template for the microbiological tests. For the cytotoxicity test, the same procedure was employed, but the samples were cut in 6 cm^2.

2.8.1. Microbial permeability

The ability of the membranes to prevent microbial penetration was tested based on Wittaya-Areekul & Prahsam [19] modified method. Briefly, the membranes were placed on open vials containing 50 mL of Tryptic Soy Broth medium (Acumedia, Neogen, Michigan) and held in place with PVC connections material sterilized by 25 kGy ionizing radiation with a test area of 19.625 cm^2 (diameter 5 cm) decontaminated by UV radiation. The vials were sealed with parafilm all around the connection for the negative control, but not for the positive control and samples. The systems were exposed for 10 days under environmental conditions, and microbial growth (turbidity) was macroscopically evaluated after 0, 5, and 10 days when they were photographed.

2.8.2. Antimicrobial activity

The antimicrobial activity test of the samples was assessed using the agar diffusion method, according to Ponce, Fritz, Del Valle, & Roura [20] modified method. The zone of inhibition assay on solid media was used for determining the antimicrobial effects of films against four typical pathogens - *Escherichia coli* (ATCC 8739), *Pseudomonas aeruginosa* (ATCC 9027), *Staphylococcus aureus* (ATCC 6538) and *Candida albicans* (ATCC 10231). The membranes, previously decontaminated, were placed on Antibiotic n.11 medium (HiMedia Laboratories, Mumbai, India) in agar plates, which had been prior seeded with 5 mL of inoculums containing approximately 10^6 CFU mL^{-1} of tested microorganisms. The plates were then incubated at 37 °C for 24 h (bacteria) or

25 °C for 48 h (yeast) and, afterward, examined for the width of inhibition. The diameter of the inhibitory zone surrounding the film discs as well as the contact area of these with the agar surface was precisely measured. Each assay was performed in duplicate.

2.8.3. Cytotoxicity

Cells were cultured in D10 medium: DMEM (Gibco®, EUA) supplemented with 10% (v/v) FBS (Vitrocell, Brazil), 1% L-Glutamine, and 1% antibiotic solution (10,000 UI.mL^{-1} penicillin, 10 mg mL^{-1} streptomycin and 1 mg mL^{-1} amphotericin B). The cells were incubated at 37 °C in a 5% CO_2 atmosphere with controlled humidity. The culture medium was changed every 2–3 days. The cultures were used for testing within 3–10 passages from the initial passage.

The cytotoxicity assay was performed according to ISO 10993-5 [21], and the samples were cut to prepare an extract according to ISO 10993-12 [22] of 0.1 g mL^{-1} at 37 °C, for 24 h, 48 h, and 72 h. The prepared extracts were diluted (100–6.25% w/v) and placed at 96 well plates seeded with murine fibroblasts Balb/c 3T3 clone A31 (ATCC® CCL¬163™) for 48 h.

After exposure, cells were carefully washed with PBS and incubated for 3 h with DMEM containing MTT 0.5 mg mL^{-1}(Invitrogen Thermo Fisher Scientific). The supernatant was then removed, and ice-cold isopropanol (Synth A1078.01BJ) was added to solubilize the formazan formed. The microplate was then shaken for 10 min in the dark. Once the ideal extraction time was standardized, extracts from dressings samples were also evaluated in HaCat cells (immortalized human keratinocytes) and L929 (mouse fibroblasts), 1 × 10^4 cells per well, for 24 h and 48 h of exposure. MTS tetrazolium salt and an electron coupling reagent (phenazine methosulfate, PMS) were applied as a vital dye, and the absorbance was measured at 490 nm for MTT and 570 nm for MTS (Synergy HTC Biotek). Culture medium was added to the cell control wells, and hospital-grade brown latex tourniquets were chosen as a positive control of the assay [23] in the proportion suggested by ISO 10993-5 [21] of 200 mg mL^{-1}.

2.8.4. Cell adhesion and proliferation

Discs of 1.4 cm^2 of each sample were arranged in plates of 24 wells and a suspension of 5 × 10^5 L929 cells per 100 μL was added in the center of a metal ring allocated on the discs. After 4 h of cell seeding, a triplicate of each sample was transferred to a new plate, washed 3 times with PBS, and then 600 μL of MTS was added to verify cell adhesion and viability. The volume was distributed in plates of 96 wells and read in a plate spectrophotometer.

Other replicas were fixed and submitted to fluorescence analysis for confirmation of adherence. Each triplicate was fixed in 4% formaldehyde (in PBS) for 10 min at room temperature. Triton X-100 0.2% solution (in PBS) was added for 7 min, and then PBST (PBS + 0.05% Tween 20 + 10% SFB) was added, and the plates maintained for 30 min in incubation. Each sample was incubated for 10 min with Alexa Fluor 488 phalloidin (0.2 μg mL^{-1}), followed by incubation for another 10 min with DAPI (0.1 μg mL^{-1}). Three cycle washes were performed with PBS between each stage mentioned. The same procedure was performed after 5 days of cultivation to verify proliferation.

The samples were evaluated under a fluorescence confocal microscope (Leica) connected to an imaging system (LasX software - Leica DMI 8), in defined and pre-selected fields, the methodology also used for all specimens (method " tilescan xyz"), reading in λEx358 nm and λEm461nm (DAPI) and λEx495nm and λEm518 nm (Alexa Fluor). The 3D reconstruction was performed after obtaining the focal planes of total restoration in 94.16 μm thick with 60 slices, in 24 fields.

2.9. Statistic analysis

The results obtained were submitted to the mean calculations, standard deviation, and coefficient of variation. Subsequently, they were evaluated by multi-factor variance analysis (ANOVA) at a significance level of 95% (α = 0.05). The results were submitted to the Tukey test, for significance analysis between the means, with the significance level of 1 and 5%.

3. Results and discussion

3.1. Development of the dressings

The freeze-drying technique leads to dressings with satisfactory interconnected porosity [9]. It allows the remotion of the water used in the production of the samples, keeping the temperature low enough for the polymeric region do not dissolve and constitutes an efficient mechanical resistance to prevent pore collapse during the drying process [24].

When a chemical cross-linker is added to the sample, covalent bonds are the main interactions that form the networks, but this does not exclude other interactions such as hydrogen bridges and hydrophobic interactions. However, covalent bonds increase and become predominant as the density of crosslinking increases [5]. Therefore, it is possible to infer that the EPI R sample has predominantly covalent bonds. At the same time, EPI NR, due to the previously neutralization process, may present proportions of covalent and ionic interactions.

Liu et al. [18] developed an injectable chitosan hydrogel. The gelling mechanism is based on the acetic acid neutralization by sodium bicarbonate, which generates a three-dimensional polymer network by physical junctions, resulted from the deprotonation of -NH3+ in chitosan. Such an easy and effective technique which produces a three-dimensional network and helps us to explain the results found in the present study.

In the pH change, ionized NH_3^+ groups are deprotonated in NH_2, favoring a crosslinking like effect, by the disappearance of ionic repulsion, that is, forming hydrophobic hydrogen interactions. Thus, $NaHCO_3$ is suggested as a three-dimensional network formation agent in chitosan, that is, a cross-linker-like agent, with the formation of physical junctions that accompany the gradual neutralization between HCO_3^- and acetic acid [11,25]. Treated in alkaline medium, chitosan forms networks between chains, dispensing with the use of a recticuling agent [11,26].

In the obtaining process of the QUI NR sample, only the solution of sodium bicarbonate, by immersion and subsequent washing, was efficient in generating a porous and sufficiently resistant material. The use of an ecologically and biologically compatible reagent resulted in a material with benefits comparable to those produced with ionic liquids, besides simplicity as an additional advantage. Fig. 1 provides a representation of the process.

3.2. Physicochemical characterization

The comparison of FTIR spectra shows chemical reactions or even interactions between chitosan and cross-linker or between chitosan and neutralizing agent (Fig. 2). The broad peak between 3200 and 3450 cm^{-1}, approximately, is consistent with the overlay of the stretch of O-H hydrogen bonds, NH_2 asymmetric stretch, and NH stretch involving hydrogen bonds [6,27,28]. This broad peak is visible in all of the four samples, as it is characteristic of the chitosan. The peak seems at 3441 cm^{-1} corresponds to NH_2 and OH vibrational elongation [29]. The stretching between 2880 and 2970 cm^{-1} refers to CH. Moreover, the peak at 2868 cm^{-1} in all samples is related to the stretching vibration of this connection and the aliphatic groups -CH2 and -CH3, could also be observed for all the samples [7].

The band at 1650 cm^{-1} corresponds to amide I [27] in the acetylated units of chitosan, while 1586 cm^{-1} [6] results from the overlapping from the vibration of amide II and the deformation of primary amines in the deacetylated units [6,27]. At 1320 cm^{-1}, elongation is attributed to C-N in secondary amide (amide III) [27]. Comparing QUI R with samples neutralized by sodium bicarbonate (QUI NR and EPI NR), a

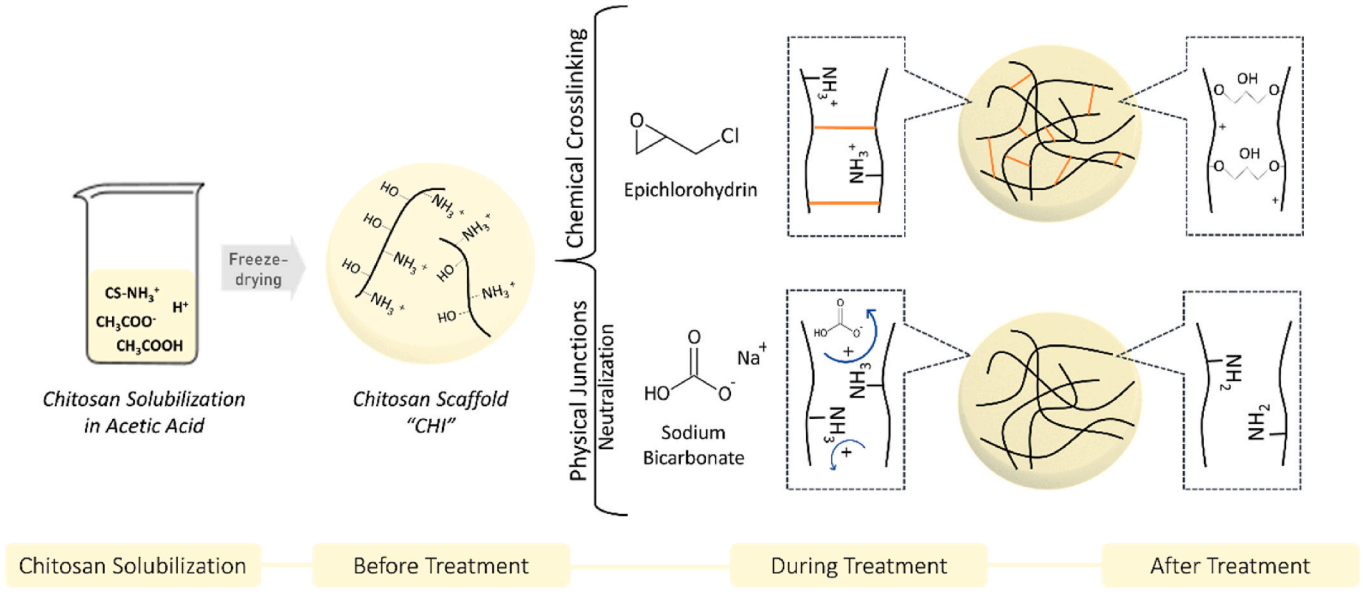

Fig. 1. Graphic representation of the interactions generated by the treatments of the dressings. In orange are represented the covalent bonds made with the addition of Epichlorohydrin. The blue arrows indicate the displacement of an H^+ proton caused by bicarbonate treatment. (For interpretation of the references to color in this figure legend, the reader is referred to the Web version of this article.)

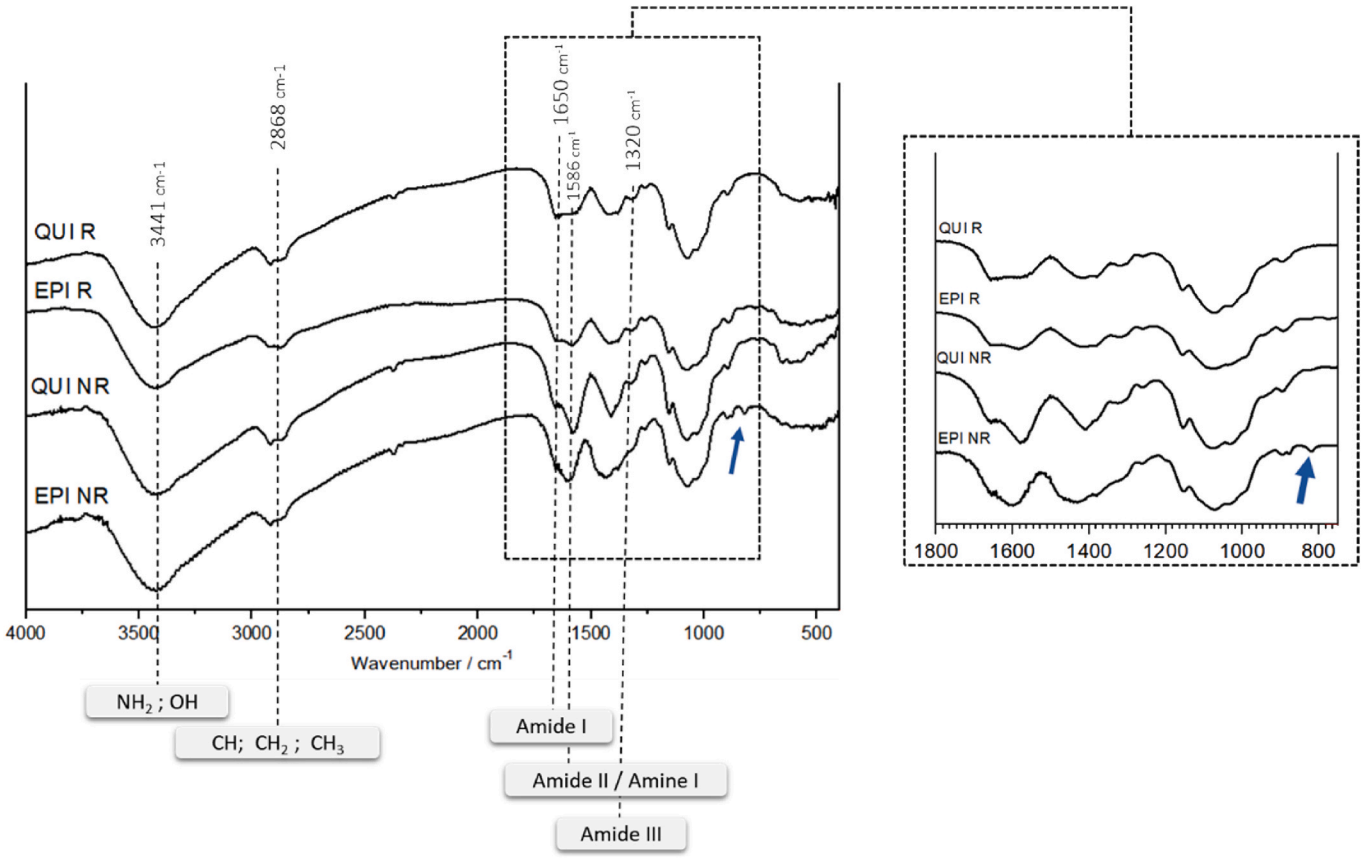

Fig. 2. FTIR spectra of chitosan dressings. Detail on the right illustrating length from 750 to 1800 cm^{-1} where the main events occur. The arrow indicates the peak related to the epoxy group for the EPI NR sample.

displacement of the wavenumber of amide I was noted and the intensity of the O-H elongation vibrations became relatively lower compared to amide II and amide III in protonated chitosan (QUI R). This can be attributed to NH_2 protonation and suggests that the neutralization process was effective.

Epoxy ring rupture and removal of chlorine from Epichlorohydrin, result in carbon atoms that bind to the hydroxyl groups of chitosan carbon 6 [8]. The peaks C-Cl (700–800 cm^{-1}) or epoxy group peaks (915 cm^{-1}) that suggest the presence of remnants of Epichlorohydrin [30] were not observed for the EPI R sample, supporting the occurrence

of successful covalent reticulation. However, for EPI NR, the peak, indicated by the arrow in Fig. 2, is observed.

Concerning the EPI NR sample, neutralization with sodium bicarbonate was performed before the addition of Epichlorohydrin, promoting crosslinking like-effect, probably due to physical junctions, which modified the conformation of chitosan chains. Thus, chemical crosslinking with Epichlorohydrin by covalent bonds in the polymer chain possibly was hampered. The epoxy group peak (915 cm^{-1}) from the unreacted epichlorohydrin was observed in the EPI NR, which was not found for the EPI R sample.

Thermal stability, degradation behavior and structure of chitosan samples were investigated. The thermograms are illustrated in Fig. 3, where endothermic peaks of the DSC with mass loss (TG) is indicative of loss of adsorbed water while the decomposition corresponds to exothermic peaks.

The first mass loss of the samples occurred from about 25 to 150 °C with a higher mass loss for QUI R (16.46%), followed by EPI NR (11.73%), while EPI R and QUI NR presented very close rates (9.79% and 9.69%). These peaks are attributed to water loss. The endothermic peak shifted to a higher temperature when there is the ability to interact with the hydroxyl group of the polymer, difficulting the water removal [31].

The residual humidity of the samples, evaluated on a moisture analyser, ranged from 18.353% for EPI NR to 27.285% for EPI R (Table 1), with no significant difference between the means values. These results corroborate those found by TG and DSC techniques, since the endothermic peaks, related to the loss of water from the samples, did not present statistical difference between them.

The material humidity for wound dressing is a crucial issue since if it is too low, it can extract moisture from the lesion and hinder epithelial cell migration, delaying the healing process and leaving less uniform scars [32].

The degradation corresponding to exothermic peaks in DSC, stage in which the highest mass losses (TG) occurred, exhibited peak temperatures of 292 °C (QUI R), 273 °C (QUI NR), 295 °C (EPI R) and 257 °C (EPI NR). The highest peak, found for EPI R, could be related to covalent bonds from the chemical crosslinking to which the sample was submitted. Deng et al. [27] associated the mass loss above 300 °C with the released energy by the chitosan pyrolysis, which is initiated by random breaks of glycosidic bonds followed by additional degradation and elimination of volatile products, causing exothermic events in the DSC curve.

The start temperature (T_{onset}) of the cross-linked samples was higher the QUI R (control), which could be related to the increased resistance of the materials when submitted to the treatments.

The thermogravimetric analysis, up to 700 °C, showed the lowest residual mass for QUI R (27.51%) and the highest for EPI NR (33.49%). EPI R and QUI NR samples presented very similar results, 31.81%, and 31.12%, respectively (Suppl. Table 1). The residues are compounds that were not degraded up to 700 °C. Additional tests up to 900 °C, under the air atmosphere, were carried out (Suppl. Fig.1); no residues were found for QUI R, EPI R, and EPI NR samples. However, EPI NR still presented residues (7.49%), probably from inorganic material. Sodium from the neutralization step may have been entrapped in the structure by the

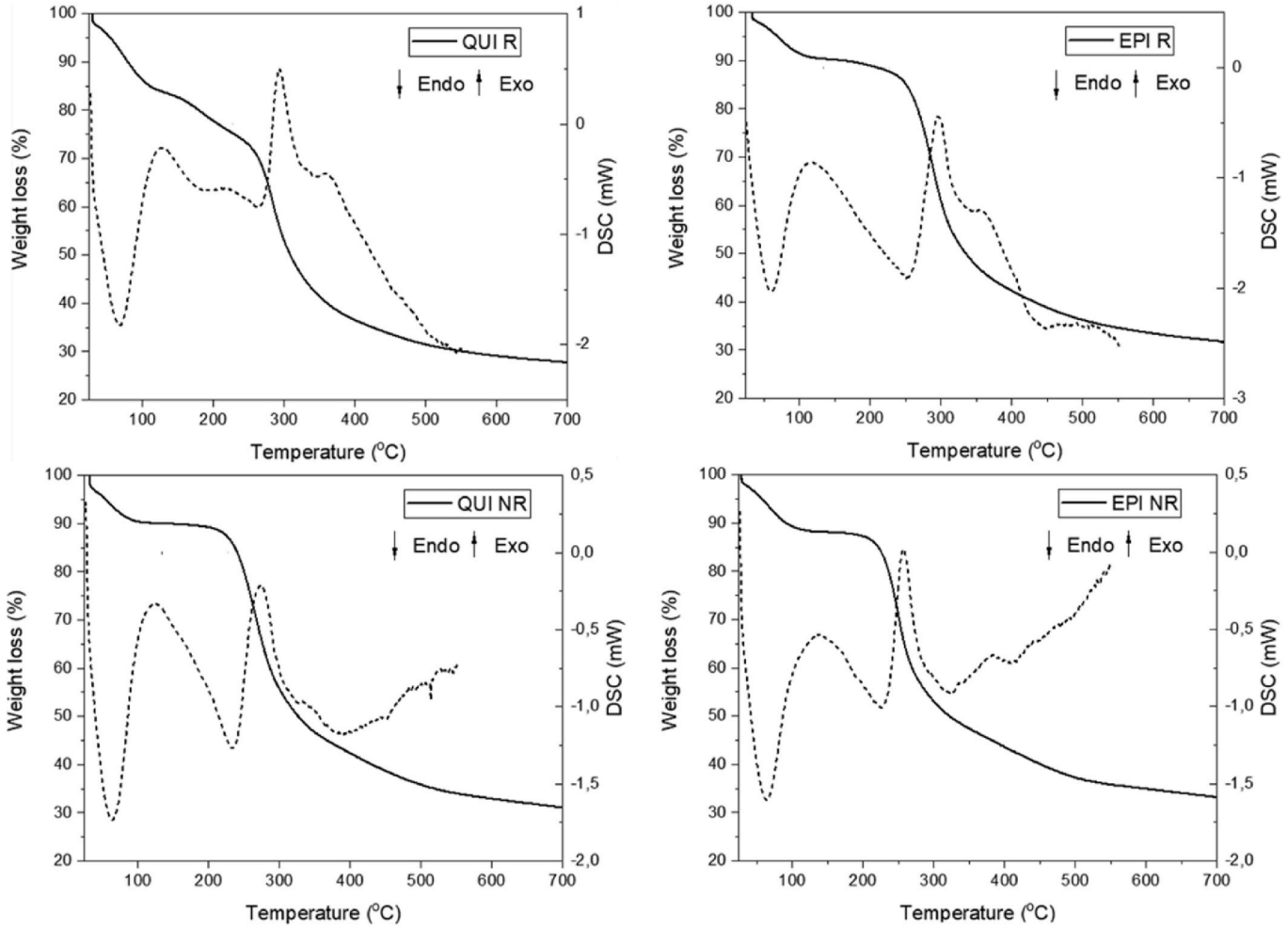

Fig. 3. Thermal analysis (DSC and TG) of chitosan dressings under the nitrogen atmosphere (Solid line: TG; Dashed line: DSC).

Table 1
Thickness, Residual Moisture, WVP, SFP, and Swelling Properties of QUI R, EPI R, QUI NR, and EPI NR dressings. On the right, graphical representation of the values indicated in each line. Significance level: **: 1%; *: 5%. Equal letters indicate that there is no difference between the means in the significance level indicated by the asterisks.

			QUI R		EPI R		QUI NR		EPI NR	
	Thickness (mm)		0,19±0,03		1,59±0,60		1,71±0,18		2,23±0,17	
	Residual Moisture (%)		22,64±1,47	a	27,29±9,55	a	21,25±0,68	a	18,35±1,53	a
Water Vapor Permeation	Total Mass Gain of the Systems (g)	**	0,29±0,01	ab	0,24±0,01	b	0,24±0,01	b	0,31±0,04	a
	Water Vapor Transmission Rate (g/m^2.24h)	**	360,23±17,35	ab	295,66±7,45	b	292,51±7,35	b	390,29 ±47,82	a
	Water Vapor Permeation Capacity (g.mm/24h.m^2.kPa)	**	35,11±1,69	c	109,57±2,76	b	103,95±2,61	b	188,23 ±23,06	a
Simulated Fluid Permeation	Fluid Permeation Rate (g/24h.m^2)	**	16505,27 ±11566,89		2234,00 ±110,12	a	1966,75 ±153,56	b	1695,08 ±48,98	c
	Fluid Absorption Capacity in 24h (g/24h.m^2)	**	833,21±266,30		681,63 ±83,14	a	483,43 ±40,17	ab	598,78 ±87,22	c
	Fluid Movement Capacity (g/24h.m^2)	**	17338,48 ±11429,47		2915,63 ±75,88	a	2450,18 ±161,69	b	2293,86 ±126,39	b
Swelling Properties	Swelling Capacity - Simulated Fluid (%)	**			974,66 ±277,53	a	929,00 ±283,75	a	1454,49 ±5,60	a
	Swelling Capacity - PBS (%)	**			1155,56 ±231,91	a	886,67 ±308,89	a	1493,33 ±277,63	a
	Swelling Capacity - D10 (%)	**			1121,11 ±210,35	a	1072,22 ±72,75	a	1405,56 ±217,57	a

cross-linking step. Such additional tests confirmed that the residues under the nitrogen atmosphere were carbonaceous compounds since they were oxidized in the air.dressing.

3.2.1. *Scanning electron microscopy*

In general, crosslinking provided homogeneity of the dressings when compared to the control, QUI R, which presents filamented structures, observed in the cross-sectional section (Fig. 4B). In the first step of the production of the dressings, common to all samples and prior to treatments for crosslinking, lyophilization maintains the polymeric structure achieved by freezing the chitosan solution in plates. For the QUI R sample, in which no reticulating or neutralizing solutions were used, the process generates clogging of the pores of the initial structure, so the difference in thickness of this sample compared to those treated (Fig. 4), and absence of pores on the surface (Fig. 4 A).

The EPI R and QUI NR samples (Fig. 4C, D and E, F, respectively), exhibit similar characteristics, with well-distributed pores that connect by well-defined and structured walls promoting resistance. It is also evident the larger thickness, when compared to the control, QUI R (Fig. 4 and Supplement. Fig 2).

When the cross-sectional area obtained by the fracture (Fig. 4D, 4F and 4H) is observed, the QUI NR sample exhibits laminar profile, while those treated with Epichlorohydrin exhibit sinuous aspect, due to covalent crosslinking, however, EPI NR has a more open network than EPI R.

A biomaterial should have high and interconnected porosity, and a wide surface area that allows the installation of high cell density and promotes neovascularization when implanted *in vivo* [24]. These pores must be structured, with open geometry and with adequate size [33]. In view of this, the physical structure of the dressings obtained by the three treatments have potential for application in the treatment of wounds.

3.3. *Water vapor permeability*

All the results obtained in tests to characterize the samples dressing are summarized in Table 1.

When the water vapor flow is evaluated at 24 h through the samples area, given by the Water Vapor Transmission Rate (WVTR), the samples relate in the same way (Table 1). The highest value found for NR PPE may be related to the characteristic of more open pores, as observed by SEM (Fig. 4), while the lower values, including that found for the samples that receives the chemical reticulator (EPI R), present the pores more closed and, therefore, are more structured. QUI R contains cracks that may have facilitated vapor permeation, while the treated samples allow the diffusion of free molecules due to the increase in free volume caused by pores. When considering the thickness of the dressing samples and steam pressure, obtaining the Water Vapor Permeability (WVP), QUI R starts to present the lowest value (Table 1), due to the more compacted morphology observed in SEM, the sample offers lower permeability.

EPI R and QUI NR presented, respectively, WVTR of 295.7 and 292.5 g m^{-2}.day^{-1}, values corresponding to those of a human skin under normal conditions, ranging from 215 to 350 g m^{-2} per day [34]. EPI NR exhibited higher value, but of the same magnitude. The parameters are related to efficiency in maintaining a damp wound or avoiding dryness of the wound, so the three treatments resulted in dressings with adequate characteristics when compared to those describe in the literature.

3.4. *Fluid handling capacity and swelling degree*

The wound moisture must be prudently managed for optimal wound healing rates. The changes in the wound moisture and the moisture skin around the wound can determine the healing process. If the wound is too dry, the healing may delay or impair, while the excess fluid can bring on maceration or infection. Therefore, the optimal healing environment is settled by applying a convenient dressing that is removed in time to prevent maceration or adherence.

The fluid handling capacity (FHC) is defined as the sum of the Moisture Vapor Transmission Rate (MVTR) and the Absorbency (ABS), The MVTR and ABS are related to the exudate production and wound moisture, respectively, and they are considered to select the appropriated dressing.

The EPI R presented the highest MVTR, followed by the QUI NR and EPI NR samples. The QUI-R samples did not show sufficient strength to perform these tests due to the dressing rupture and SEF leakage after a

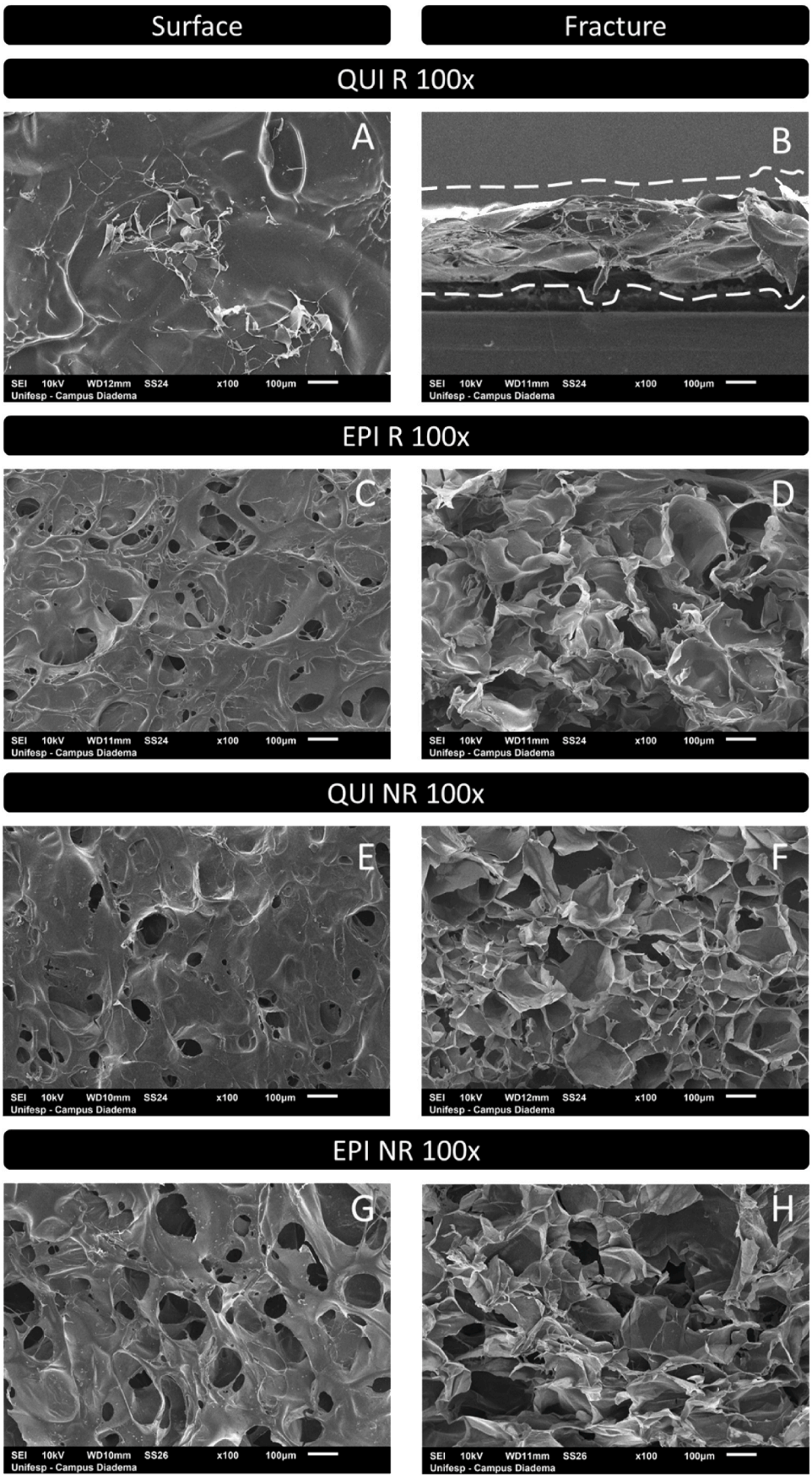

Fig. 4. Scanning Electron Microscopy of the samples, at 100x. Images on the left: surface of samples. Images on the right: fracture performed with exposure to liquid nitrogen, cross-sectional.

few hours, showing that cross-linking is crucial for the solubility and mechanical resistance.

The water loss by evaporation from the skin is usually 204 ± 12 g/m^2/24 h, but ranges from 279 ± 26 to 5138 ± 26 g/m^2/24 h for injured skin, depending on the severity of the lesion. A dressing for exudative wounds should present MVTR from 2000 to 2500 g/m^2/24 h, allowing the removal of excess exudate without risk of causing dehydration to the wound [41]. EPI R and QUI NR results are among this range (Table 1), while EPI NR has a value slightly below the recommended value for MVTR and can be considered for injuries with reduced production of physiological liquids. According to Thomas and Young [35], the MVTR was 1.67 and 12.35 g/10cm^2/24 h (1670 and 12350 g/m^2/24 h), respectively, for ActivHeal and Allevyn Adhesive, which means that MVTR values can present a wide range. In this way, the MVTR values found in our work were like commercial dressing such as ActivHeal.

The wound dampness or dryness is related to the Absorbency of the dressings, despite the evaporation. Absorbency is used to decide how damp or dry the wound has to be kept. EPI R and EPI NR present statistical difference, presenting the highest and lowest value, respectively, while the Absorbency of QUI NR is between them (Table 1). These data are consistent with the endothermic peaks of the DSC, which is related to the water retention capacity of the samples. However, the absorbances found in the present work were much smaller than those found for commercial dressing by Thomas and Young [35] and chitosan films by Kimura et al. [36]. It must be considered that commercial dressings usually have many layers of different materials, which can affect barriers properties; moreover, the grammage and thickness of the dressings have to be also considered for comparison. Unfortunately, these last properties were not provided in both works.

Amino groups on chitosan dressings could be protonated or deprotonated depending on pH. In an aqueous medium of pH 7, almost all NH_2 groups would be deprotonated, and may eventually form hydrogen bonds, thus chitosan would present a low load density, causing changes in the behavior of swelling, influenced only by the osmotic pressure gradient. When the fluid enters the polymer network, the NH_2 and OH groups of chitosan form hydrogen bonds internally and externally, which increases the cross-linking density of the network dressing [30]. The EPI R and EPI NR presented the highest absorption capacity value due probably to the incorporation of OH groups in crosslinking, as observed by Cao et al. [37] dressing for cross-linked chitosan films with epichlorohydrin, which increased hydrophilicity.

The Fluid Handling Capacity (FHC) describes how much fluid passes through the dressings considering which part is retained in them. EPI R presented the highest FHC; on the other hand, EPI NR and QUI NR did not show any statistical difference between them (Table 1). There is a lack of scientific papers about FHC. For Kimura et al. [36] and Debone et al. [38], FHC ranged approximately between 2 and 6 g/10cm^2/24 h (2000 and 6000 g/m^2/24 h), while ATKINS observed FHC ranging from 10000 to 24000 g/m^2/24 h. Chitosan spongy materials are solid structures capable of absorbing up to more than 20 times their dry mass due to their microporosity, which provides good cellular interaction, and wound healing, by absorbing wound exudates helping tissue regeneration [1].

It is mentioned that the so-called physical junctions, derived from ionic interaction, because they are reversible connections, generally provide weak mechanical properties and are likely to be dissolved more easily, while chemical reticulations improve mechanical properties by reducing dispersion [6]. In the present work, tests that exposed the samples directly to the simulated fluid indicated very close results for the QUI NR and EPI R samples, and neither of the two samples collapsed or dissolved.

The use of simple absorbent dressings can lead to dehydration of the outer surface of the wound, which can make it devitalized, and form a barrier to the migration of epidermal cells from the wound margin. This barrier causes migratory cells to penetrate deeper into the dermis to reach closure, prolonging healing time due to the increasing in the loss of healthy tissue [14]. Thus, wounds that are kept moist heal faster than those kept dry.

The pores of chitosan dressings adsorbed solvent molecule, which can generate changes in pH and lead to degradation or solubilization in the swelling medium [39].

The chemical crosslinking of dressings, unlike the non-reticulated ones, generates a permanent porous structure that allows the free diffusion of water by improving the mechanical properties of the material produced [6]. Ionic crosslinking builds a three-dimensional polymer network by neutralizing chitosan easily and effectively, without the addition of solvents and other chemical substances [11].

In 20 min, the samples QUI R, EPI R, QUI NR and EPI NR presented high fluid absorption capacity, approximately 24x, 10x, 9x and 14x the value of their initial mass, respectively. If the proportion of water that composes the final formulation (swelled) compared to the initial (dry) formulation is considered, 95.9% (±0.50), 90.2% (±2.92), 89.8% (±2.83) and 93.6% (±0.02) of fluid in the final composition, are obtained.

The first evaluation that the test allows to perform, is the structural integrity of the dressings as soon as they are put in contact with the fluid, and in the process of subsequent dehydration. The QUI R sample presents a gelation process just minutes after the contact with the liquid, unlike the other samples, which maintained structural integrity. This characteristic was expected, as it is known that chitosan membranes have the disadvantage of being fragile, justifying the crosslinking used to optimize the strength of the material, and allow bridges to form between the polymer chains [2].

Rapid swelling (first 10 min of assay) was observed for all samples, and this behavior is typical of highly hydrophilic materials and/or that have great pore interconnectivity, which allows a rapid circulation of nutrients throughout [9,30].

QUI NR and EPI R presented a similar dehydration profile and obtained the lowest free water loss speed values, keeping the fluid in its matrix for longer (Supplement. Fig. 4). The observed result may be related to the structure of these two frameworks, which is more closed compared to the NR EPI, as observed in SEM. This characteristic is quite remarkable because, from the perspective of use as a dressing, these structures will maintain the moisture needed to heal the wound for longer. An ideal dressing should quickly absorb the excess exudate excreted by the wound, and avoid dehydration, creating an ideal environment of moisture for tissue repair [40].

Gel fraction higher values also demonstrate the profile closeness of EPI R (93.71%) and QUI NR (93.29), followed by EPI NR (84.63) and QUI R (88.24%). As corroborated by Stanescu et al. [16], the percentages of gel fraction found were higher for cross-linked samples.

There is no statistical difference between the swelling of the dressings in fluid, D10 and PBS allowing comparison of data in the validation of assays that have been performed in different liquids (Table 1).

Chitosan presents solubility in acid aqueous solutions, so, in the QUI R sample, a possible residual acetic acid content may have favored swelling while promoting the dissolution and rupture of the material [1,5,6,9] intensified due to the dressing sample being protonated, reinforcing the need for treatment with neutralizers for samples made with this polymer in acid medium. Because of this, as expected, the QUI R sample gave way to the fluid leaking all the liquid resulting in extremely higher values. Another hypothesis, yet to be proved, is that the NH3+ groups, when in the presence of water are quickly and intensely solvated, contributing to the dissolution of the polymeric chains of chitosan. As there was no crosslinking in this sample, the tendency is that the polymer chains gain mobility and consequently the 3d structure of the dressing sample is lost. These data were not considered for sample comparison (Table 1).

3.5. Mechanical properties

Uniaxial mechanical properties are important for maintaining

material integrity during handling, transportation, storage, etc. In this sense, the puncture force is a useful parameter for analysis of resistance of materials in the form of film [15,41,42]. The use of a material that is resistant to rupture, but flexible and malleable, favors multi-functionality, enables local procedures such as puncture for biological sampling, suture, or even injection of drugs if there is a need and injection on the material for application of mesenchymal stem cells, for example.

The characteristics of force and displacement until rupture were important to delineate the mechanical properties of the samples in question, but, above all, to provide comparison data between the treatments performed in chitosan dressings.

Once again, QUI NR and EPI R showed no statistical difference (Fig. 5). They presented lower resistance to perforation and greater elongation (or deformation distance) when swelled compared to dry samples, a result also observed by Remunan-Lopez et al. [43]. As expected, the swelled samples showed lower resistance, given by lower rupture force values than the dry ones, and greater distance until rupture, a parameter related to stretching. The water molecules act by collapsing the physical bridges, decreasing the network density, thus an elongation and a decrease in tensile strength was observed in the swollen samples [16].

Characteristics and physical properties of films can be modified with the incorporation of organic acids, which can promote a plasticizing effect to the material due to inter-polymeric interactions promoted by hydroxyl groups. Thus, attributes such as thickness, permeability to water vapor, and also, the resistance to perforation, can be changed [41]. The non-neutralized QUI R sample showed higher resistance, but the rupture profile, different from that found for the other samples, corresponded to a break or tear. Although fractions of the most homogeneous samples were selected to enable the assay, this is not the frequent condition of QUI R, which presents cracks, ripples, etc. The result can also be explained by the more compact morphology, evidenced by SEM and it is necessary to force until rupture, contrary to EPI NR, with the network more open, much lower strength was required.

EPI R showed higher values in the mechanical strength test (force to rupture), in the DSC related to degradation by the TG curve (exothermic peak) and in the Simulated Fluid Handling Capacity test, when compared to EPI NR. These results, corroborated the difference found between the two samples in the FTIR, show the structural difference generated by the neutralization process with $NaHCO_3$ prior to epichlorohydrin reticulation.

The literature reports that mixtures of chitosan with other substances are necessary for the development of an adequate material for tissue engineering, since chitosan has its fragility as a major limitation [44]. It is known that chemical crosslinking agents provide a greater mechanical resistance to materials due to the formation of covalent bonds between the polymer chains of chitosan molecules [7,17,30,31,37,45]. However, the result obtained leads to the understanding that, in this case, the chemical crosslinking agent is expendable. Treatment with sodium bicarbonate, when compared to treatment with Epichlorohydrin, constitutes a procedure strategy that is much less harmful to the environment, with the use of less toxic reagents, and more financially economical.

3.6. *In vitro degradation*

In vivo degradation of biodegradable polymers into smaller fragments can occur both by the performance of biological entities, such as cells, microorganisms, and enzymes, as well as by hydrolysis, free radical action, ionic species, and water components [6].

Lysozyme degrades chitosan [46,47] hydrolyzing the β bond (1–4) between N-acetylglucosamine and glucosamine in chitosan or chitin. However, according to the distribution of the N-acetyl group, the chitin has more residues of N-acetyl glucosamine, lysozyme has more significant action on it [48]. For this reason, the degradation of low-molar mass chitosan occurs more rapidly [6].

There are two degradation mechanisms for polymers when implanted in biological systems [6,49]. Bulk Erosion (Fig. 6A) generates random fragmentation by hydrolysis of the chains, reducing the molecular weight of the material due to the diffusion of water into the polymer structure resulting in material loss throughout the matrix volume and the device collapses after erosion to a critical degree. This is the case of QUI R, whose degradation gives very fragmented material. Surface Erosion (Fig. 6A) promotes a volume loss of the structure making it thinner or smaller, without changing the molecular weight of the polymer inner block, as it involves hydrolytic cleavage of the material surface chains, and the rate of water intrusion into its structure is slow compared to the erosion process. This type of degradation occurred for EPI R, QUI NR, and EPI NR, which maintained a monolithic structure, not losing shape throughout the trial. On the other hand, QUI R

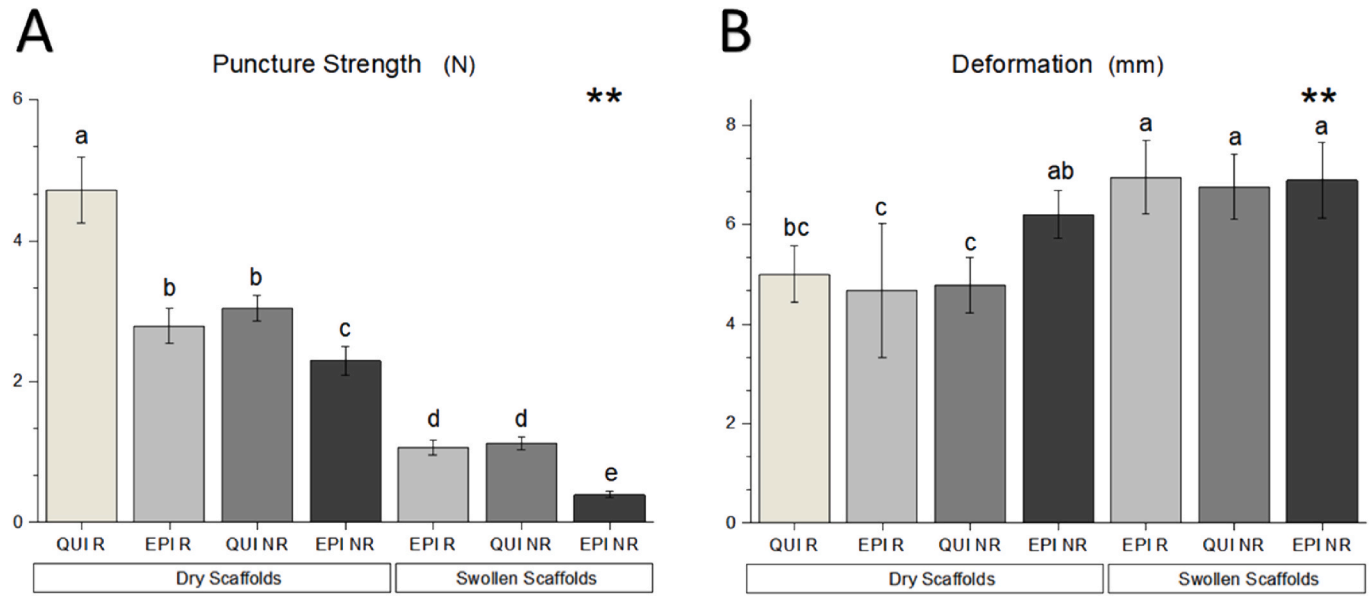

Fig. 5. Mechanical strength analysis of dry and swelled Dressings: A: for rupture force and B: as for rupture distance. Legend: significance level: **: 1%. Equal letters indicate that there is no difference between the means in the significance level indicated by the asterisks.

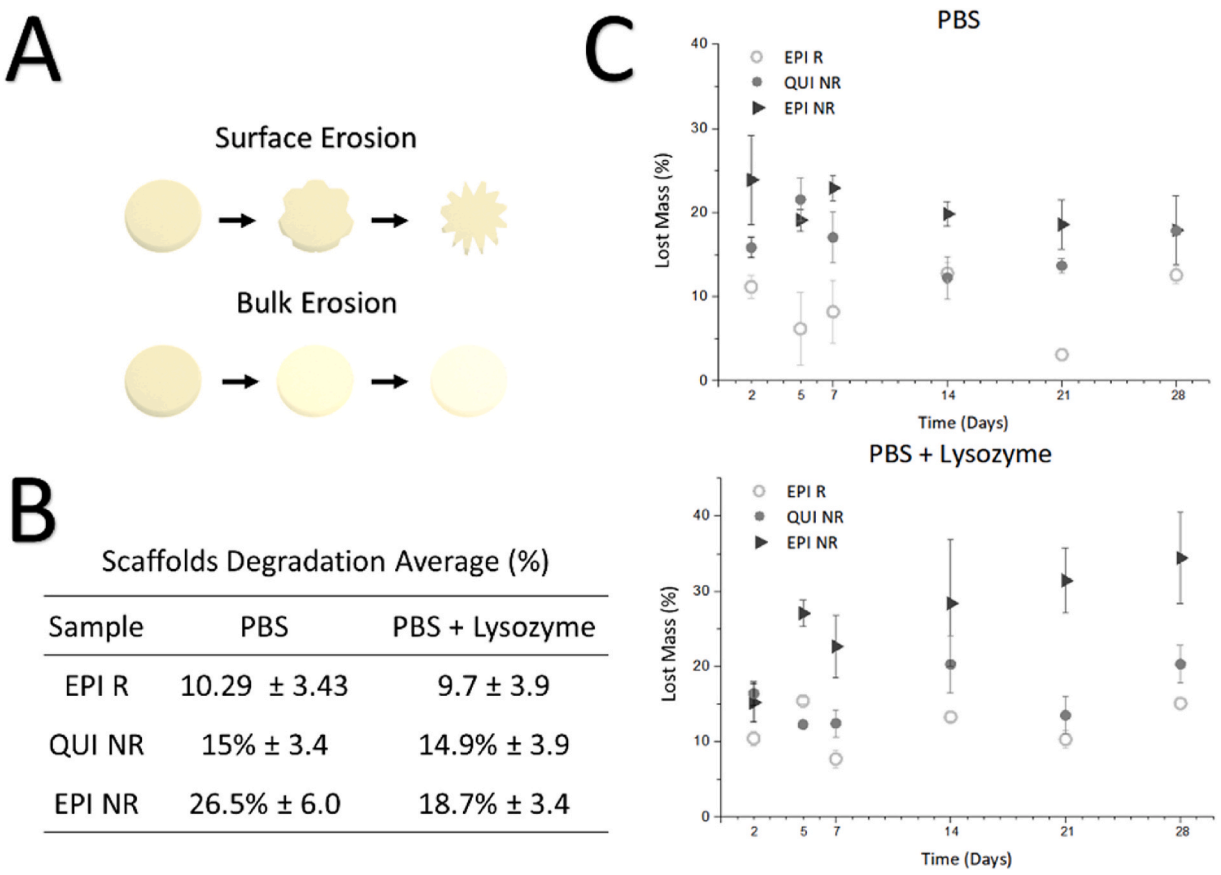

Fig. 6. Biodegradation analysis *in vitro*. A: graphic representation of two types of erosions, based on Edlund & Albertsson [49] B: Degradation average of dressings. C: Percentage of Degradation of Dressings in PBS Solution and PBS Solution with Human Lysozyme.

presented integral degradation in most experimental times, and the percentage of small mass in the initial times.

It was observed that in both media, PBS (Fig. 6A) and PBS/Lysozyme (Fig. 6B), the mass loss was higher for EPI NR. Also, such loss was more significant in the presence of the enzyme, demonstrating the protease's catalytic activity even in carbohydrate hydrolysis, as already confirmed by Hirano et al. (1989). The EPI R and QUI NR samples showed very similar results, practically overlapping. The neutralization process facilitated the lysozyme activity due to the compounds' removal that obstructs the access of the enzyme.

Dressings must have a degradation rate that coincides with the tissue regeneration rate, although there is no established criterion or related norm [44]. EPI R, QUI NR, and EPI NR have the potential for biomedical application in biological systems, due to the need to preserve the structure of the dressings during the cell filling process. Also, if the degradation is speedy, the accumulation of amino-saccharides can generate an inflammatory response [6].

Histological tests imply that the extracellular matrix secreted by growing cells on dressings can improve the mechanical property of the material, providing greater flexibility. On the other hand, this fact leads to the extracellular matrix occupying spaces within the samples and may reduce porosity [47]. A dressing should serve as a support for cells, which proliferate and, during tissue synthesis, produce the extracellular matrix while the dressing degrades [17]. The biodegradable characteristic of chitosan is advantageous since the material can initiate degradation before the extracellular matrix secreted by the cells obstructs all the pores present in the material, being able to be replenished and allowing gas exchange and pore availability for irrigation.

Lysozyme is naturally present in the injury fluid, and the fact that chitosan is depolymerized by this enzyme and N-acetyl glycosaminidase, ensures the delayed release of N-acetyl glucosamine monomers and glucosamine in the healing process, sugars involved in re-epithelialization and necessary for biosynthesis of hyaluronic acid and other components of the extracellular matrix by fibroblasts [50]. This happens due to these degradation products that stimulate macrophages and initiate fibroblast proliferation, collaborating with collagen deposition and stimulating the natural synthesis of hyaluronic acid at the wound site [51].

3.7. Antimicrobial activity and permeability

Although the mechanism is not fully elucidated, the literature reports that chitosan exhibits antimicrobial activity [52] and several hypotheses have been proposed based on its cationic nature [2,4,52]. Although the antimicrobial effects of chitosan have been reported in the literature against *Candida albicans*, *Enterobacter cloacae*, *Enterococcus faecalis*, *Escherichia coli*, *Klebsiella pneumoniae*, *Pseudomonas aeruginosa*, *Staphylococcus aureus* and *Streptococcus pyogenes* [2], no inhibition halos were observed in the dressings trial. The result does not invalidate their use, as it does not affect the local microbiota, which may contribute to healing in some circumstances [53].

All vials and negative controls in the microbial penetration test remained clear, while all positive controls showed visible turbidity (Supplement. Fig. 5 and Fig. 6), indicating that the medium was suitable for microorganism growth, and that they did not overcome the barrier formed by dressings between the external and internal environment. Result was confirmed by absorbance reading (Supplement. Fig. 7).

Infection is one of the main challenges in wound treatment and, therefore, it is expected that the dressing can maintain an appropriate environment with interface that favors wound healing but avoids contamination. If occlusive, the dressing may not be permeable, while some materials may be porous enough to drain exudates from the wound

but not to prevent the penetration of microorganisms [54]. Therefore, the results found in the microbial permeation assay, added to the vapor and fluid permeation test, express a satisfactory evaluation to enable the application of the materials studied as dressings.

The tubes containing BHI medium and samples after UV exposure were clear and comparable to negative controls and no CFU was observed after incubation in plates with TSA, indicating efficacy of the decontamination methodology adopted.

3.8. Citotoxicity

QUI R was ruled out in the preliminary pH test, based on Ruphuy et al. [9], which considers the alteration of the color of the culture medium containing phenol red, as a criterion for excluding samples because it indicates pH deviation from the optimal interval (7.2–7.4).

The cytotoxicity test is the measurement of the effect of a substance on cells during exposure [55]. In accordance with ISO 10993-5 [21] the maximum limit for the material to be considered safe is 70% cell viability. The cell viability data were shown in Fig. 7.

The extracts of the dressings obtained in 24 h, 48 h and 72 h, exposed to Balb/3T3 fibroblasts, were not considered cytotoxic, however, the extraction time of 24 h manifests a more reliable result because it ensures that extract components have not been degraded in longer extraction periods, therefore, it was defined as the extraction pattern. The extracts of the samples were exposed to HaCat (human keratinocytes) and L929 (murine fibroblasts), this time varying the time of exposure of the extracts to the cells. None of the samples showed cytotoxicity at none of the exposure times, while positive control compromised cell viability almost completely, indicating that the cells of both assays were responsive. Thus, it was possible to guarantee the safety of the three samples, EPI R, QUI NR and EPI NR, in the three cell types.

3.9. Adhesion and proliferation

The immune system reaction, proliferation and differentiation cell activation promote repair of physical tissue damage, seeking the replacement of original functional capacities and preservation of integrity, which is an essential ability of the body [56].

In the 3D reconstruction of fluorescence images (Fig. 8) it is possible to observe a clear difference between the exposure times of 4 h (Supplement. Videos A, C and E) and 5 days (Supplement. Videos B, D and F), indicating cell adhesion and proliferation by the extension of the 3 dressings.

Supplementary video related to this article can be found at https://doi.org/10.1016/j.matchemphys.2023.127636

It is worth remembering that the samples also absorb D10 medium (Section 3.5) ensuring nutrition of adhered cells, and provide support for long-term cell growth and proliferation, as evaluated in the degradation assay.

Biocompatibility with organism is related to the ability of the material to generate minimal allergic, inflammatory, or toxic reactions when in contact with living tissues or organic fluids, implying that this material has a favorable response in the specific application [6,57]. The material surface properties have a great effect on its biocompatibility, since cells perform their physiological functions on it [44].

The use of Epichlorohydrin in the EPI R sample configures the addition of an extrinsic chemical reagent to biological systems, and, as for EPI NR, leaching of this crosslinking should be better evaluated. QUI NR is basically composed of chitosan, a biocompatible polymer, and treated with sodium bicarbonate, present in biological systems. From this perspective, the QUI NR sample offers less risk possibilities to the biological system and, added to the physicochemical characteristics very close to those found for the covalently reticulated sample (EPI R), this dressing provides greater advantage considering the risk-benefit of the three formulations compared, inferring that the chemical crosslinking, in this case, would be expendable.

4. Conclusion

Treatment with $NaHCO_3$ in QUI NR is less drastic when compared to crosslinked dressings with Epichlorohydrin, as covalent reticulation involves more reagents in development, and leaching should be considered in the risk-benefit assessment of these samples. In fact, FTIR analyses demonstrated the possibility of EPI NR containing free Epichlorohydrin in the composition, due to the reduced action of this reagent due to the network conformation having been previously altered with the physical junctions formed in neutralization. The characteristics of EPI R and QUI NR, including mechanical resistance, are statistically comparable, arguing that chemical covalent reticulation may be dispensable. Both have satisfactory physicochemical characteristics, pore structure with sufficient size and distribution to build a balance between exudate absorption and water loss, facilitating cell migration and increasing re-epithelialization, and dressing degradation would occur while the wound would become less exudative. Microbiological assays have indicated that both offer wound protection against external pathogens without harming the skin's natural microbiota. Since the three dressings showed application potential and adequate characteristics, the risk-benefit analysis should be based on factors such as methodology, reagents employed, and reproducibility. The development of QUI NR is controlled, safe and simple, as it involves reagents that are

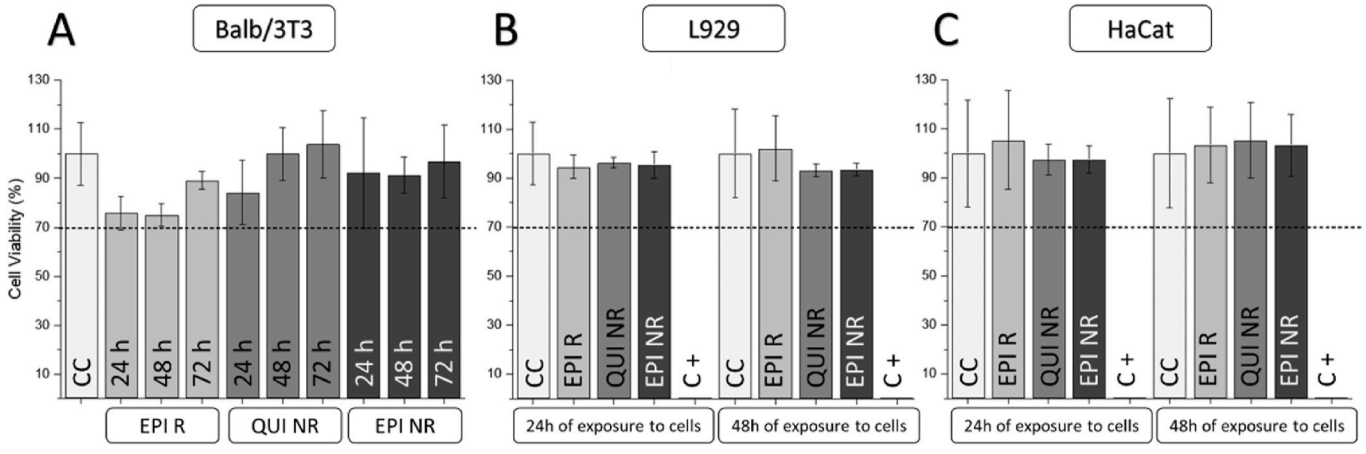

Fig. 7. Cellular viability expressed as a percentage (%) cell control (CC) using extracts from dressings samples. C+ is positive control. A: Viability of balb/3T3 cells exposed to 24 h, 48 h and 72 h extracts. B and C: Cell viability of L929 (B) and HaCat (C) cells exposed to 24 h extracts during 24 and 48 h of assay for dressings samples.

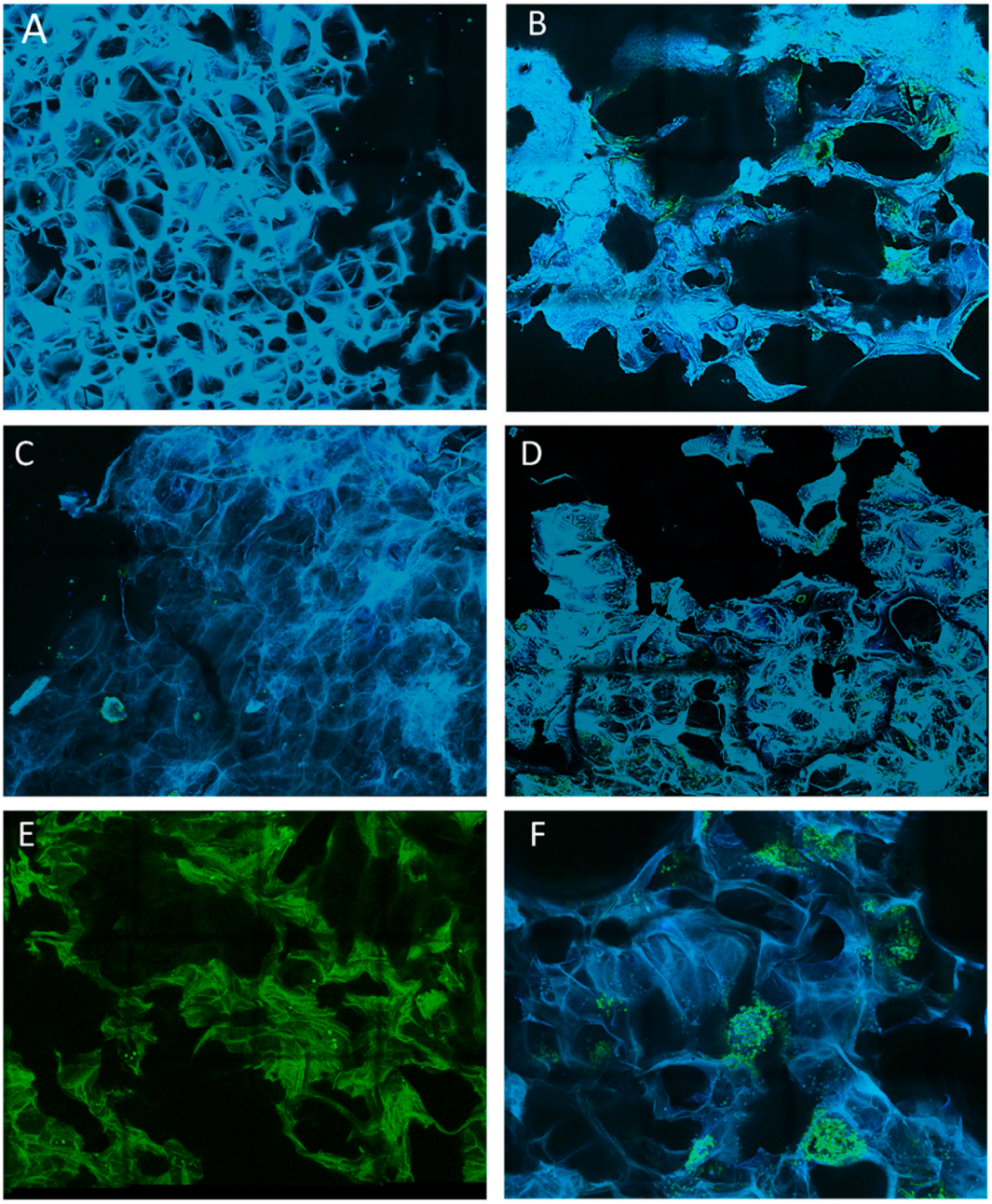

Fig. 8. Cells labeled with DAPI and Alexa Fluor 488 increase by 200x. A: EPI R 4 h. B: EPI R 5 days. C: QUI NR 4 h. D: QUI NR 5 days. E: EPI NR 4 h. F: EPI NR 5 days.

easy to handle, financially viable, and generate washing residues that are not harmful to the environment, evidencing the potential of application as a biodressing.

Funding

This research did not receive any specific grant from funding agencies in the public, commercial, or not-for-profit sectors.

Data references

Portal to access the intellectual asset of Universidade Federal de São Paulo (UNIFESP – Institutional Repository): http://repositorio.unifesp.br/?locale-attribute=en.

CRediT authorship contribution statement

Julia Vaz Ernesto: Formal analysis, Investigation, Data curation, Writing – original draft, Writing – review & editing. **Ísis de Macedo Gasparini:** Investigation. **Fúlvio Gabriel Corazza:** Investigation. **Mônica Beatriz Mathor:** Resources. **Classius Ferreira da Silva:** Formal analysis, Resources, Writing – original draft, Writing – review & editing. **Vania Rodrigues Leite-Silva:** Resources, Writing – review & editing. **Newton Andréo-Filho:** Formal analysis, Resources, Writing – original draft, Writing – review & editing. **Patricia Santos Lopes:** Formal analysis, Investigation, Resources, Data curation, Writing – original draft, Writing – review & editing, Supervision, Project administration, Funding acquisition.

Declaration of competing interest

The authors declare that they have no known competing financial interests or personal relationships that could have appeared to influence the work reported in this paper.

Data availability

Data will be made available on request.

Acknowledgment

We would like to thank Capes for the Master's scholarship and the kind help on performing analysis from Dr. Cristina Yoshida, Dr. Tereza Martins and Dr Alison Chaves and all technicians who are part of the UNIFESP Research and Teaching Instrumentation Center. We also would like to thank FAPESP for the Cientific Initiation Scholarship, that begins this work (FAPESP 2015/20440-0).

Appendix A. Supplementary data

Supplementary data to this article can be found online at https://doi.org/10.1016/j.matchemphys.2023.127636.

References

[1] F. Croisier, C. Jérôme, Chitosan-based biomaterials for tissue engineering, Eur. Polym. J. 49 (2013) 780–792, https://doi.org/10.1016/j.eurpolymj.2012.12.009.
[2] M. Rodríguez-Vázquez, B. Vega-Ruiz, R. Ramos-Zúñiga, D.A. Saldaña-Koppel, L. F. Quiñones-Olvera, Chitosan and its potential use as a scaffold for tissue engineering in regenerative medicine, BioMed Res. Int. 201AD (2015) 1–15, https://doi.org/10.1155/2015/821279.
[3] H. Ueno, M. Murakami, M. Okumura, T. Kadosawa, T. Uede, T. Fujinaga, Chitosan accelerates the production of osteopontin from polymorphonuclear leukocytes, Biomaterials 22 (2001) 1667–1673, https://doi.org/10.1016/S0142-9612(00)00328-8.
[4] M. Dash, F. Chiellini, R.M. Ottenbrite, E. Chiellini, Chitosan - a versatile semi-synthetic polymer in biomedical applications, Prog. Polym. Sci. 36 (2011) 981–1014, https://doi.org/10.1016/j.progpolymsci.2011.02.001.
[5] J. Berger, M. Reist, J.M. Mayer, O. Felt, N.A. Peppas, R. Gurny, Structure and interactions in covalently and ionically crosslinked chitosan hydrogels for biomedical applications, Eur. J. Pharm. Biopharm. 57 (2004) 19–34, https://doi.org/10.1016/S0939-6411(03)00161-9.
[6] M.J.C. Moura, Preparação e Caracterização de Hidrogéis de Quitosano para Administração por Via Injetável, Universidade de Coimbra, 2014.
[7] M.J. Moura, H. Faneca, M.P. Lima, M.H. Gil, M.M. Figueiredo, In situ forming chitosan hydrogels prepared via ionic/covalent Co-cross-linking, Biomacromolecules 12 (2011) 3275–3284, https://doi.org/10.1021/bm200731x.
[8] V.L. Gonçalves, M.C.M. Laranjeira, V. Fávere, V. Drago, Liberação de ferro (iii) de microesferas reticuladas de quitosana, Visão Acadêmica 6 (2005) 15–24.
[9] G. Ruphuy, M. Souto-Lopes, D. Paiva, P. Costa, A.E. Rodrigues, F.J. Monteiro, C. L. Salgado, M.H. Fernandes, J.C. Lopes, M.M. Dias, M.F. Barreiro, Supercritical CO $_2$ assisted process for the production of high-purity and sterile nano-hydroxyapatite/chitosan hybrid scaffolds, J. Biomed. Mater. Res. B Appl. Biomater. (2017), https://doi.org/10.1002/jbm.b.33903.
[10] Q. He, Q. Ao, Y. Gong, X. Zhang, Preparation of chitosan films using different neutralizing solutions to improve endothelial cell compatibility, J. Mater. Sci. Mater. Med. 22 (2011) 2791–2802, https://doi.org/10.1007/s10856-011-4444-y.
[11] L. Liu, X. Tang, Y. Wang, S. Guo, Smart gelation of chitosan solution in the presence of NaHCO3for injectable drug delivery system, Int. J. Pharm. 414 (2011) 6–15, https://doi.org/10.1016/j.ijpharm.2011.04.052.
[12] E. Assaad, M. Maire, S. Lerouge, Injectable thermosensitive chitosan hydrogels with controlled gelation kinetics and enhanced mechanical resistance, Carbohydr. Polym. 130 (2015) 87–96, https://doi.org/10.1016/j.carbpol.2015.04.063.
[13] C.M.P. Yoshida, E.N. Oliveira, T.T. Franco, Chitosan tailor-made films: the effects of additives on barrier and mechanical properties, Packag. Technol. Sci. 22 (2009) 161–170, https://doi.org/10.1002/pts.839.
[14] S. Thomas, Fluid Handling Properties of Hydrogel Dressings, Wound Management Communications - BST Publications, 2007.
[15] I. Leceta, P. Guerrero, K. De Caba, Functional properties of chitosan-based films, Carbohydr. Polym. 93 (2013) 339–346, https://doi.org/10.1016/j.carbpol.2012.04.031.
[16] P.O. Stanescu, I.C. Radu, R. Leu Alexa, A. Hudita, E. Tanasa, J. Ghitman, O. Stoian, A. Tsatsakis, O. Ginghina, C. Zaharia, M. Shtilman, Y. Mezhuev, B. Galateanu, Novel chitosan and bacterial cellulose biocomposites tailored with polymeric nanoparticles for modern wound dressing development, Drug Deliv. 28 (2021) 1932–1950, https://doi.org/10.1080/10717544.2021.1977423.
[17] M. Alizadeh, F. Abbasi, A.B. Khoshfetrat, H. Ghaleh, Microstructure and characteristic properties of gelatin/chitosan scaffold prepared by a combined freeze-drying/leaching method, Mater. Sci. Eng. C 33 (2013) 3958–3967, https://doi.org/10.1016/j.msec.2013.05.039.
[18] J.G. dos S. Batista, Desenvolvimento de Matrizes Poliméricas Biodegradáveis à base de Quitosana e possíveis Blendas como Sistemas de Liberação Controlada de Fármacos, Instituto de Pesquisas Energéticas e Nucleares - Autarquia Associada a Universidade de São Paulo, 2015, https://doi.org/10.11606/D.85.2016.tde-18022016-145449.
[19] S. Wittaya-Areekul, C. Prahsarn, Development and in vitro evaluation of chitosan-polysaccharides composite wound dressings, Int. J. Pharm. 313 (2006) 123–128, https://doi.org/10.1016/j.ijpharm.2006.01.027.
[20] A.G. Ponce, R. Fritz, C. Del Valle, S.I. Roura, Antimicrobial activity of essential oils on the native microflora of organic Swiss chard, LWT - Food Sci. Technol. (Lebensmittel-Wissenschaft -Technol.) 36 (2003) 679–684, https://doi.org/10.1016/S0023-6438(03)00088-4.
[21] International Standard ISO 10993-5 Biological Evaluation of Medical Devices - Part 5: Tests for Cytotoxicity: in Vitro Methods, 2009.
[22] ISO, Biological evaluation of medical devices — Part 12: sample preparation and reference materials. https://doi.org/10.1109/IEEESTD.2007.4288250, 2012.
[23] E.S. Lourenço, J. Côrtes, J. Costa, A. Linhares, G. Alves, Evaluation of commercial latex as a positive control for in vitro testing of bioceramics, Key Eng. Mater. 631 (2014) 357–362. https://10.4028/www.scientific.net/kem.631.357.
[24] M.-H. Ho, P.-Y. Kuo, H.-J. Hsieh, T.-Y. Hsien, L.-T. Hou, J.-Y. Lai, D.-M. Wang, Preparation of porous scaffolds by using freeze-extraction and freeze-gelation methods, Biomaterials 25 (2004) 129–138, https://doi.org/10.1016/S0142-9612(03)00483-6.
[25] Q. Wu, M. Maire, S. Lerouge, D. Therriault, M.-C. Heuzey, 3D printing of microstructured and stretchable chitosan hydrogel for guided cell growth, Adv Biosyst 1 (2017), 1700058, https://doi.org/10.1002/adbi.201700058.
[26] Y. Xu, D. Xia, J. Han, S. Yuan, H. Lin, C. Zhao, Design and fabrication of porous chitosan scaffolds with tunable structures and mechanical properties, Carbohydr. Polym. 177 (2017) 210–216, https://doi.org/10.1016/j.carbpol.2017.08.069.
[27] A. Deng, X. Kang, J. Zhang, Y. Yang, S. Yang, Enhanced gelation of chitosan/β-sodium glycerophosphate thermosensitive hydrogel with sodium bicarbonate and biocompatibility evaluated, Mater. Sci. Eng. C 78 (2017) 1147–1154, https://doi.org/10.1016/j.msec.2017.04.109.
[28] R.C. Silva, M.A.S. Andrade Jr., A.R. Cestari, Adsorção de Cr(VI) em esferas reticuladas de quitosana: novas correlações cinéticas e termodinâmicas utilizando microcalorimetria isotérmica contínua, Quim. Nova 33 (2010) 880–884, https://doi.org/10.1590/S0100-40422010000400022.
[29] S. Wrobel, S.C. Serra, S. Ribeiro-Samy, N. Sousa, C. Heimann, C. Barwig, C. Grothe, A.J. Salgado, K. Haastert-Talini, *In vitro* evaluation of cell-seeded chitosan films for peripheral nerve tissue engineering, Tissue Eng. 20 (2014) 2339–2349, https://doi.org/10.1089/ten.tea.2013.0621.
[30] I.M. Garnica-Palafox, F.M. Sánchez-Arévalo, C. Velasquillo, Z.Y. García-Carvajal, J. García-López, C. Ortega-Sánchez, C. Ibarra, G. Luna-Bárcenas, L. Solís-Arrieta, Mechanical and structural response of a hybrid hydrogel based on chitosan and poly(vinyl alcohol) cross-linked with epichlorohydrin for potential use in tissue engineering, J. Biomater. Sci. Polym. Ed. 25 (2014) 32–50, https://doi.org/10.1093/jxb/ert298.
[31] H.S. Tsai, Y.Z. Wang, Properties of hydrophilic chitosan network membranes by introducing binary crosslink agents, Polym. Bull. 60 (2008) 103–113, https://doi.org/10.1007/s00289-007-0846-x.
[32] K.Y. Lee, D.J. Mooney, Alginate: properties and biomedical applications, Prog. Polym. Sci. 37 (2012) 106–126, https://doi.org/10.1016/j.progpolymsci.2011.06.003.
[33] L. Baldino, S. Cardea, I. De Marco, E. Reverchon, Chitosan scaffolds formation by a supercritical freeze extraction process, J. Supercrit. Fluids 90 (2014) 27–34, https://doi.org/10.1016/j.supflu.2014.03.002.
[34] Y. Tu, M. Zhou, Z. Guo, Y. Li, Y. Hou, D. Wang, L. Zhang, Preparation and characterization of thermosensitive artificial skin with a Sandwich structure, Mater. Lett. 147 (2015) 4–7, https://doi.org/10.1016/j.matlet.2015.01.163.
[35] S. Thomas, S. Young, Exudate-handling mechanisms of two foam-film dressings, 309–315, https://doi.org/10.12968/JOWC.2008.17.7.30524, 2013.
[36] V.T. Kimura, C.S. Miyasato, B.P. Genesi, P.S. Lopes, C.M.P. Yoshida, C.F. Da Silva, The effect of andiroba oil and chitosan concentration on the physical properties of chitosan emulsion film, Polímeros 26 (2016) 168–175, https://doi.org/10.1590/0104-1428.2013.
[37] W. Cao, M. Cheng, Q. Ao, Y. Gong, N. Zhao, X. Zhang, Physical, mechanical and degradation properties, and Schwann cell affinity of cross-linked chitosan films, J. Biomater. Sci. Polym. Ed. 16 (2005) 791–807, https://doi.org/10.1163/1568562053992496.
[38] L.S. Estevam, H.S. Debone, C.M.P. Yoshida, C.F. Da Silva, Adsorption of Bovine Serum and Bovine Haemoglobin onto Chitosan Film, Brazilian Meeting on Adsorption (EBA9), Recife, Brazil, 2012.
[39] T. Debnath, S. Ghosh, U.S. Potlapuvu, L. Kona, S.R. Kamaraju, S. Sarkar, S. Gaddam, L.K. Chelluri, Proliferation and differentiation potential of human adipose-derived stem cells grown on chitosan hydrogel, PLoS One 10 (2015), e0120803, https://doi.org/10.1371/journal.pone.0120803.
[40] G. Lu, K. Ling, P. Zhao, Z. Xu, C. Deng, H. Zheng, J. Huang, J. Chen, A novel in situ-formed hydrogel wound dressing by the photocross-linking of a chitosan derivative, Wound Repair Regen. 18 (2010) 70–79, https://doi.org/10.1111/j.1524-475X.2009.00557.x.

[41] C.A. Campos, L.N. Gerschenson, S.K. Flores, Development of edible films and coatings with antimicrobial activity, Food Bioprocess Technol. 4 (2011) 849–875, https://doi.org/10.1007/s11947-010-0434-1.
[42] P. Cazón, M. Vázquez, G. Velazquez, Composite films of regenerate cellulose with chitosan and polyvinyl alcohol: evaluation of water adsorption, mechanical and optical properties, Biol. Macromol. (2018), https://doi.org/10.1016/j.ijbiomac.2018.05.148.
[43] C. Remunan-Lopez, R. Bodmeier, C. Remuñán-López, R. Bodmeier, C. Remunan-Lopez, R. Bodmeier, C. Remuñán-López, R. Bodmeier, Mechanical, water uptake and permeability properties of crosslinked chitosan glutamate and alginate film, J. Contr. Release 44 (1997) 215–225, https://doi.org/10.1016/S0168-3659(96)01525-8.
[44] F. Han, Y. Dong, Z. Su, R. Yin, A. Song, S. Li, Preparation, characteristics and assessment of a novel gelatin-chitosan sponge scaffold as skin tissue engineering material, Int. J. Pharm. 476 (2014) 124–133, https://doi.org/10.1016/j.ijpharm.2014.09.036.
[45] A. Aryaei, A.H. Jayatissa, A.C. Jayasuriya, Nano and micro mechanical properties of uncross-linked and cross-linked chitosan films, J. Mech. Behav. Biomed. Mater. 5 (2012) 82–89, https://doi.org/10.1016/j.jmbbm.2011.08.006.
[46] J.-K. Francis Suh, H.W.T. Matthew, Application of chitosan-based polysaccharide biomaterials in cartilage tissue engineering: a review, Biomaterials 21 (2000) 2589–2598, https://doi.org/10.1016/S0142-9612(00)00126-5.
[47] J. Mao, L. Zhao, K. De Yao, Q. Shang, G. Yang, Y. Cao, Study of novel chitosan-gelatin artificial skin in vitro, J. Biomed. Mater. Res. 64 (2003) 301–308, https://doi.org/10.1002/jbm.a.10223.
[48] T. Han, N. Nwe, T. Furuike, S. Tokura, H. Tamura, Methods of N -acetylated chitosan scaffolds and its in vitro biodegradation by lysozyme, J. Biomed. Sci. Eng. 5 (2012) 15–23, https://doi.org/10.4236/jbise.2012.51003.
[49] U. Edlund, A.-C. Albertsson, Degradable polymer microspheres for controlled drug delivery, Degradable Aliphatic Polyesters 157 (2002) 67–112, https://doi.org/10.1007/3-540-45734-8_3.
[50] H.S.R. Costa Silva, K.S.C.R. Dos Santos, E.I. Ferreira, Quitosana: derivados hidrossolúveis, aplicações farmacêuticas e avanços, Quim. Nova 29 (2006) 776–785, https://doi.org/10.1590/S0100-40422006000400026.
[51] R. Jayakumar, M. Prabaharan, P.T. Sudheesh Kumar, S.V. Nair, H. Tamura, Biomaterials based on chitin and chitosan in wound dressing applications, Biotechnol. Adv. 29 (2011) 322–337, https://doi.org/10.1016/j.biotechadv.2011.01.005.
[52] R.C.F. Cheung, T.B. Ng, J.H. Wong, W.Y. Chan, Chitosan: an update on potential biomedical and pharmaceutical applications. https://doi.org/10.3390/md13085156, 2015.
[53] D.N. Frank, A. Wysocki, D.D. Specht-Glick, A. Rooney, R.A. Feldman, A.L. St Amand, N.R. Pace, J.D. Trent, Microbial diversity in chronic open wounds, Wound Repair Regen. 17 (2009) 163–172, https://doi.org/10.1111/j.1524-475X.2009.00472.x.
[54] Z. Cao, X. Luo, H. Zhang, Z. Fu, Z. Shen, N. Cai, Y. Xue, F. Yu, A facile and green strategy for the preparation of porous chitosan-coated cellulose composite membranes for potential applications as wound dressing, Cellulose 23 (2016) 1349–1361, https://doi.org/10.1007/s10570-016-0860-y.
[55] L.C. Keong, A.S. Halim, In Vitro models in biocompatibility assessment for biomedical-grade chitosan derivatives in wound management, Int. J. Mol. Sci. 10 (2009) 1300–1313, https://doi.org/10.3390/ijms10031300.
[56] L. Elviri, A. Bianchera, C. Bergonzi, R. Bettini, Controlled local drug delivery strategies from chitosan hydrogels for wound healing, Expet Opin. Drug Deliv. (2016), https://doi.org/10.1080/17425247.2017.1247803.
[57] M.S. Shoichet, Polymer scaffolds for biomaterials applications, Macromolecules 43 (2010) 581–591, https://doi.org/10.1021/ma901530r.